Direct Measurement of Cell Wall Stress Stiffening and Turgor Pressure in Live Bacterial Cells

Yi Deng, Mingzhai Sun, and Joshua W. Shaevitz

Phys. Rev. Lett. **107**, 158101 — Published 6 October 2011

DOI: 10.1103/PhysRevLett.107.158101

Direct measurement of cell wall stress–stiffening and turgor pressure in live bacterial cells

Yi Deng,[1] Mingzhai Sun,[2] and Joshua W. Shaevitz[1,2,*]

[1] *Department of Physics, Princeton University, Princeton, NJ 08544, USA*
[2] *Lewis-Sigler Institute for Integrative Genomics, Princeton University, Princeton, NJ 08544, USA*

We study intact and bulging *Escherichia coli* cells using atomic force microscopy to separate the contributions of the cell wall and turgor pressure to the overall cell stiffness. We find strong evidence of power–law stress–stiffening in the *E. coli* cell wall, with an exponent of 1.22 ± 0.12, such that the wall is significantly stiffer in intact cells ($E = 23 \pm 8$ MPa and 49 ± 20 MPa in the axial and circumferential directions) than in unpressurized sacculi. These measurements also indicate that the turgor pressure in living cells *E. coli* is 29 ± 3 kPa.

Many cellular-scale processes in biology, such as cell growth, division and motility, necessarily involve mechanical interactions. Recent theoretical work in bacteria has led to a number of physically–realistic models of bacterial cells [1–3]. However, in many instances, precise, direct measurements of the mechanical properties of cellular components in live cells are lacking.

The cell envelope in most bacteria is made of one or two layers of membrane and a rigid cell wall consisting of a network of peptidoglycan (PG) polymers. These two materials serve different cellular functions. The semi-permeable plasma membrane maintains a chemical separation between the cell interior and the surrounding medium. The large concentration of solutes in the cytoplasm generates an osmotic pressure, termed turgor pressure, that pushes the plasma membrane against the cell wall. The cell wall, on the other hand, defines the cell shape and constrains the volume under turgor.

The magnitude of the turgor pressure under physiological conditions has been estimated using several techniques: by collapsing gas vesicles in rare species of bacteria [4], by AFM indentation [5, 6], and by calculating the total chemical content of the cytoplasm [7]. The estimated pressure values vary by more than an order of magnitude, from 10^4 to 3×10^5 Pa. While mechanical experiments, such as AFM indentation, are the most direct probes, separating the mechanical contributions of the wall and pressure has not been previously possible and thus these experiments may only provide an upper bound on the true turgor pressure.

Similarly, the elasticity of the cell wall has been difficult to probe in individual, live cells. Most previous mechanical measurements on the cell wall have been performed using chemically isolated walls, termed sacculi, that may be altered from the native state, or on large bundles of cells. Yao *et al.* reported an anisotropic elasticity of 25 MPa and 45 MPa in the axial and circumferential directions relative to a cell's rod-shape using single flattened *E. coli* sacculi adhered to a substrate [9]. Thwaites and coauthors probed the elastic modulus of macroscopic threads of many *Bacillus subtilis* sacculi in humid air and found that the modulus varied from 10 to 30 MPa depending on the humidity and salt concentration [10–12]. Mendelson *et al.* measured the relaxation of single bent *Bacillus subtilis* filaments and determined the modulus to be 50 MPa [8]. Attempts to probe whole–cell elasticity have also been made using AFM indentation of *Myxococcus xanthus* cells [13] and optical–tweezer bending of *Borrelia burgdorferi* cells [14].

In addition, because the PG material is essentially a cross-linked polymer mesh, it is expected to exhibit a substantial amount of stress–stiffening [15–19]. Unpressurized sacculi thus provide a poor platform for estimating the wall elasticity in live cells. Boulbitch *et. al.* modeled the cell wall as a deformable hexagonal mesh and predicted a load-dependent elasticity with a power–law stress–stiffening exponent of about one [20]. Thwaites and coauthors found about an order of magnitude change in the thread modulus upon loading, although it is unclear how to interpret measurements from these very large, multi–sacculus objects performed in air [10–12].

Mechanical indentation of live cells is likely the most direct method for probing these sorts of mechanical properties. Under external perturbation, however, the cell wall and turgor pressure have mixed contributions to the response, making it hard to independently estimate these two quantities. By studying a bulging strain of *E. coli*, we are able to simultaneously determine both the wall elasticity and the turgor pressure and reveal their dependence [Fig. 1].

Briefly, we first obtain the turgor pressure of individual bulging cells from the bulge radius and indentation stiffness using AFM and fluorescence microscopy [Fig. 1(a-e)]. Then, from the size and stiffness of the cell body, we are able to extract the elasticity of the cell wall under tension using numerical methods. The variation in turgor pressure among bulging cells allows us to probe the mechanical properties of the PG over a broad range of stresses. Additional experiments using non–bulging cells yields the turgor pressure and wall modulus of *E. coli* under physiological conditions. More details regarding the experimental procedures are described in the supplemental materials [21].

Several lines of evidence indicate that the cell wall in

bulged cells is not significantly different than in non–bulged cells. First, bulging is a discrete event that is completed within a few seconds. Second, the cell stiffness remains constant in the presence of vancomycin until the sudden bulging event when the stiffness drops dramatically [Fig. 1(f)]. Taken together, these indicate that the mechanical properties of the cell wall as a whole are unaffected by drug treatment except at the precise location of fracture and bulging.

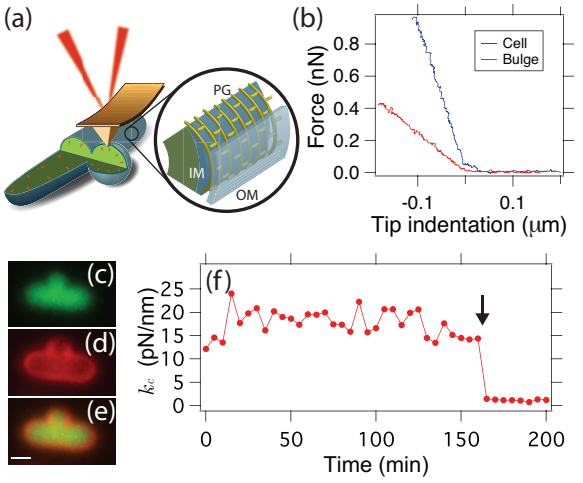

FIG. 1. (a) Schematic cartoon illustrating the bulging *E. coli* and AFM stiffness measurement. The magnified region shows the details of the inner membrane (IM), peptidoglycan (PG) network and the outermembrane (OM). (b) Typical force-indentation traces obtained by indenting a cell and bulge. (c) Cytoplasmic GFP (green) is able to occupy both the cell and bulge interiors, indicating the ability of protein–sized objects to transverse the pore. (d) A membrane stain (FM4-64, red) labels the outer membrane. (e) Overlay of the cytoplasmic EGFP and membrane stain. Scale bar is 1 μm. (f) Cell stiffness shows little variation before the bulging event (arrow) at which point it drops suddenly.

GFP molecules are able to move between the bulge and the cell interiors [Fig. 1(c)], indicating that cytoplasmic objects smaller than at least 3–4 nm are free to exchange between these compartments. Because the turgor pressure overwhelmingly results from the concentration of small solutes, the pressure in the cell and bulge can be considered the same. We calculate this pressure from the stiffness of the bulge by modeling the bulge as a liquid vesicle and the shape of the AFM tip as a cone [21].

Briefly, the total indentation size for an indentation force F, a bulge of radius R_b, an indenter half–conical angle of α and pressure P is given by [21]

$$\begin{aligned} h &= h_{gobal} + h_{dent} + h_{cone}; \\ h_{global} &= R_b - \tfrac{\sigma_b}{P}\left[1 + I(\pi/2, a)\right]; \\ h_{dent} &= \tfrac{\sigma_b}{P}\left[1 - \sin\alpha - I(\pi/2 - \alpha, a)\right]; \\ h_{cone} &= \tfrac{\sigma_b}{P}\left[\left(\sqrt{\cos^2\alpha + a} - \cos\alpha\right)\cot\alpha\right] \end{aligned} \tag{1}$$

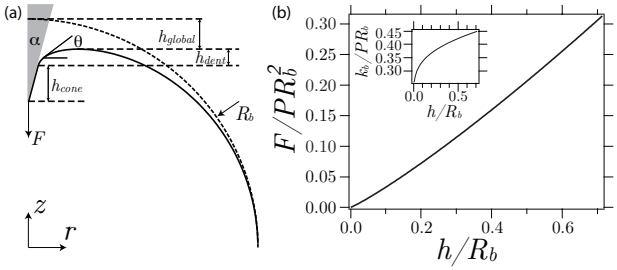

FIG. 2. Model of a fluidic membrane bulge under a force F exerted by a conical indenter. (a) The total deformation of the bulge consists of a global deformation, h_{global}, a local dent h_{dent} and the contact height h_{cone}. The dashed line is a sphere of radius equal to the bulge waist. (b) The dimensionless force–indentation relation is nearly linear. Inset: dimensionless stiffness vs. indentation.

where the bulge surface tension $\sigma_b = PR_b/2 - F/2\pi R_b$, $a = PF/\pi\sigma_b^2$, and $I(\xi, a) = \int_0^\xi \sin^2\zeta(a + \sin^2\zeta)^{-1/2}d\zeta$. The indentation, h, has a nearly linear dependence on the indentation force [Fig. 2(b)]. Under experimental conditions where $\alpha = \pi/12$, $R_b \sim 0.5\mu$m, $P \sim 1$ kPa and $F \sim 0.01 - 0.1$ nN, the dimensionless spring constant k_b/PR_b varies from 0.35 to 0.38 [Fig. 2 (b) *inset*].

For each bulging cell, we measure h/R_b and use the model to obtain the reduced stiffness k_b/PR_b as shown in the inset of Fig. 2(b). From the mechanical measurements of the bulge stiffness and radius, we then calculate the turgor pressure P in that particular cell. We then use this value to estimate the circumferential surface tension experienced by the cell wall, $\sigma_\perp = PR_c$, where R_c is the cell radius [22].

Figure 3 shows the cell radius, R_c, and stiffness, k_c, as functions of the pressure derived from bulge indentation. Both radius and stiffness are positively correlated with the turgor pressure. We further determined the size and stiffness of non–bulging cells to be 0.55 ± 0.02 μm and 0.017 ± 0.002 N/m, respectively [23].

The indentation stiffness of the cell wall is governed by terms associated with stretching and bending of the PG as well as terms related to the surface tension. While the bending energy of the wall has been shown to be negligibly small [5], we cannot ignore the stretching energy of the PG network and thus analysis of the cell indentation data is more complicated than for bulge indentation. To address this problem, we used finite–element calculations of the force–indentation relation for an inflated cylindrical shell [Fig. 4 *inset*].

Rather than attempting to estimate the elastic parameters for each measured cell, we generated a numerical model for the radius, R_c, and stiffness, k_c, in the presence of stress–stiffening and performed a global fit to all the cellular indentation data. This procedure and the fitting results are sketched below, while in depth derivations and modeling details are provided in the supplemental mate-

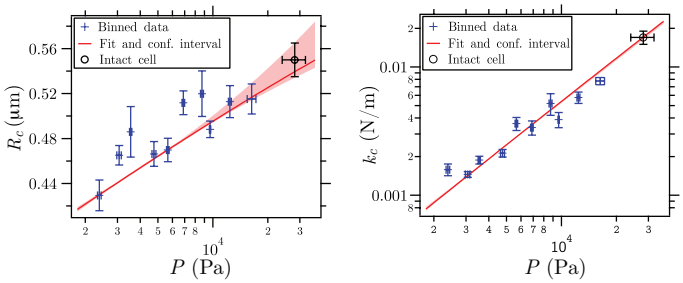

FIG. 3. Bulging cell radius R_c and indentation stiffness k_c are plotted against cell turgor pressure P. Data from 72 bulged cells are binned in 10 logarithmically–spaced bins using weights from the relative error estimates of the individual indentation traces and fluorescent images (blue crosses). Data from 42 non-bulged cells are plotted as black open squares. Red lines indicate the best fit of the stress–stiffening model along with 68% confidence intervals.

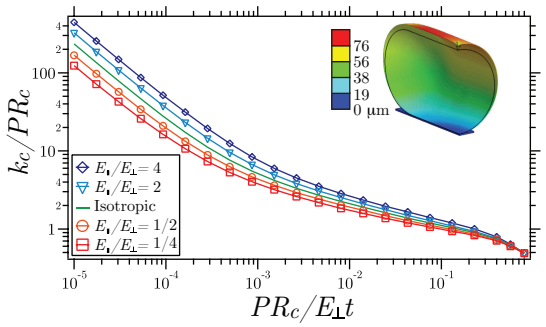

FIG. 4. Simulated value of reduced cell indentation stiffness k_c/PR_c against the reduced inflation magnitude $PR_c/E_\perp t$ for different orthotropic ratios of the stretching elasticity in the axial direction to the circumferential directions, $E_\parallel/E_\perp$. (inset) The result of a single simulation. One quadrant of the indented cylinder is shown, with color labeling the displacement in the indentation direction. The black wireframe shows the undeformed, unpressurized capsule.

rials [21].

We incorporate stress–stiffening in the cell wall by describing the nonlinear elasticity of the PG network as a power law in the turgor pressure, $E_\perp = E_0(P/P_0)^\gamma$. E_0 is the Young's Modulus at reference pressure P_0 (fixed at 5 kPa, in the middle of the range of measured bulge pressures), and γ is the stress–stiffening exponent. Here, the nonlinearity is only dependent on the pressure in a given cell and we ignore the much smaller change in stress caused by AFM indentation. The independent parameters γ and E_0t, where t is the thickness of the cell wall, fully define the nonlinear elasticity. These two quantities, combined with the radius of a cell at the reference pressure, R_0, make up the fitting parameters for interpreting bulged cells. Our global fit additionally includes the radius and stiffness data from the non–bulged, intact cells which introduces one additional free parameter: the physiological turgor pressure.

The radial expansion, $R_c(P; E_0t, \gamma, R_0)$, can be solved implicitly from the following equation as derived in the supplemental materials [21]

$$\frac{P}{P_0} = \frac{R_0}{R_c}\left[\frac{(\gamma-1)E_0t}{\gamma P_0 R_0}\left[\left(\frac{R_0}{R_c}\right)^\gamma - 1\right] + 1\right]^{\frac{1}{1-\gamma}}. \qquad (2)$$

The dimensionless quantity $PR_c/E_\perp t$ describes the magnitude of inflation under pressure.

Calculation of the cell stiffness under pressure, $k_c(P; E_0t, \gamma, R_0)$, is significantly more complicated. The dimensionless stiffness, k_c/PR_c, depends only on $PR_c/E_\perp t$ as can be found from scaling arguments [21], and monotonically decreases as the cylinder is inflated due to the relative magnitudes of surface tension and shell bending [Fig. 4 *green line*]. However, stress stiffening adds an extra complication due to an anisotropy inherent in a cylindrical geometry; the surface tension in the circumferential and axial directions of a cylinder are different by a factor of 2. Therefore, the Young's modulus, which is a function of surface tension, is orthotropic. We simulated indentation of pressurized cylinders with several different values for the elastic anisotropy, $E_\parallel/E_\perp$ [Fig. 4]. For a given pressure, the anisotropy can be calculated [21] and the correct relationship between the dimensionless stiffness and the radial inflation can be interpolated using the curves shown in Fig. 4. Combined with the radial expansion function, this is sufficient to solve for $k_c(P; E_0t, \gamma, R_0)$.

The results of a global fit of the functions $R_c(P; E_0t, \gamma, R_0)$ and $k_c(P; E_0t, \gamma, R_0)$ to the experimental data are shown in Fig. 3. The best fit yields parameter estimates of $E_0t = 0.026 \pm 0.001$ N/m, $\gamma = 1.22 \pm 0.12$, $R_0 = 464.2 \pm 0.9$ nm and a turgor pressure $P = 29 \pm 3$ kPa. At this turgor pressure, using the estimated cell wall thickness 4.5 ± 1.5 nm [6], the cell wall Young's moduli are $E_\perp = 49 \pm 20$ MPa and $E_\parallel = 23 \pm 8$ MPa.

Previous work using AFM indentation of bacteria has been used to quantify turgor pressure and cell wall elasticity [5, 6]. In that work, the relationship between linear indentation and surface tension was established, but the stretching of the cell wall was neglected or at most underestimated. Our study, which independently measures the turgor pressure and cell stiffness, suggests that cell wall stretching and surface tension contribute similar amounts to the indentation stiffness. This is most evident in the difference in the k/PR ratio for membrane bulges, ~ 0.36, and cells, ~ 0.9. This difference arises from the fluidity of lipid membranes; while the bulge can redistribute material to minimize stress, the rigid cell wall can not. For the cell wall, therefore, the overall stiffness depends on stretching even in a tension-dominated regime.

Mendelson and others introduced a pressure–independent, tube–bending method to quantify cell wall elasticity [8]. Wang *et al.* bent live *E. coli* cells and

found their flexural rigidity to be $2.0 \pm 0.4 \times 10^{-20}$ Nm^2 [24]. This result yields an axial cell wall Young's modulus, including uncertainties in the wall thickness, of $E_{\|} = 11 \pm 4$ MPa, in agreement with our measurements. Using our numerical model, we combined this value of the axial modulus with the stiffness of intact cells measured using AFM indentation and estimate the turgor pressure in intact cells to be 35 ± 7 kPa. This bulge–free measurement further validates our estimate of the turgor pressure and cell wall stress–stiffening.

Polymer networks often exhibit a nonlinear stress-strain relation due to intrinsic geometric nonlinearities and a potential nonlinear force-extension relation of the individual polymers at finite temperature [15]. Boulbitch *et. al.* modeled the PG network as a hexagonal mesh of rigid glycan subunits and elastic peptide cross-links. They predicted a power–law relationship between the axial elastic modulus and stress with a stiffening exponent of ~ 1 [20]. We find a stiffening exponent of 1.22 ± 0.12 in the *E. coli* cell wall in quantitative agreement with the model and similar to observations from gram–positive *Bacillus* sacculus threads [11].

To summarize, we used AFM and fluorescent microscopy to probe the elastic properties of live *E. coli* cells using a system that allows us to separately probe pressure and elasticity. Our results indicate that the turgor pressure in live cells is ~ 30 kPa, or ~ 0.3 atm. This value is lower than previous chemical estimates of the pressure but similar to other mechanical measurements. Our data further indicate that the cell wall stress-stiffens. Stress–stiffening affords a unique mechanical advantage to cells by preventing abrupt cell shape changes during changes in external pressure or osmolarity while maintaining a relatively compliant cell elasticity under normal conditions.

This research was supported by the Pew Charitable Trusts and NSF Award PHY-0844466. We gratefully thank Natacha Ruiz and Tom Silhavy for help in constructing cell strains and Ned Wingreen for helpful advise.

* shaevitz@princeton.edu

[1] L. Furchtgott, N. S. Wingreen, and K. C. Huang, Mol Microbiol (2011), 10.1111/j.1365-2958.2011.07616.x.
[2] S. X. Sun, S. Walcott, and C. W. Wolgemuth, Current Biology **20**, R649 (2010).
[3] H. Jiang and S. X. Sun, Phys. Rev. Lett. **105**, 028101 (2010).
[4] D. P. Holland and A. E. Walsby, Journal of Microbiological Methods **77**, 214 (2009).
[5] Phys Rev E Stat Phys Plasmas Fluids Relat Interdiscip Topics **62**, 1034 (2000).
[6] X. Yao, J. Walter, S. Burke, S. Stewart, M. H. Jericho, D. Pink, R. Hunter, and T. J. Beveridge, Colloids and Surfaces B: Biointerfaces **23**, 213 (2002).
[7] D. S. Cayley, H. J. Guttman, and M. T. Record, Biophys J **78**, 1748 (2000).
[8] N. H. Mendelson, J. E. Sarlls, C. W. Wolgemuth, and R. E. Goldstein, Phys Rev Lett **84**, 1627 (2000).
[9] X. Yao, M. Jericho, D. Pink, and T. Beveridge, J Bacteriol **181**, 6865 (1999).
[10] J. J. Thwaites and N. H. Mendelson, Proc Natl Acad Sci U S A **82**, 2163 (1985).
[11] J. J. Thwaites and N. H. Mendelson, Int J Biol Macromol **11**, 201 (1989).
[12] N. H. Mendelson and J. J. Thwaites, J Bacteriol **171**, 1055 (1989).
[13] A. E. Pelling, Y. Li, W. Shi, and J. K. Gimzewski, Proc Natl Acad Sci U S A **102**, 6484 (2005).
[14] C. Dombrowski, W. Kan, M. A. Motaleb, N. W. Charon, R. E. Goldstein, and C. W. Wolgemuth, Biophys J **96**, 4409 (2009).
[15] M. L. Gardel, J. H. Shin, F. C. MacKintosh, L. Mahadevan, P. Matsudaira, and D. A. Weitz, Science **304**, 1301 (2004).
[16] G. H. Koenderink, M. Atakhorrami, F. C. MacKintosh, and C. F. Schmidt, Phys Rev Lett **96**, 138307 (2006).
[17] R. Tharmann, M. M. A. E. Claessens, and A. R. Bausch, Phys Rev Lett **98**, 088103 (2007).
[18] C. P. Broedersz, C. Storm, and F. C. MacKintosh, Phys Rev Lett **101**, 118103 (2008).
[19] T. Kim, W. Hwang, H. Lee, and R. D. Kamm, PLoS Comput Biol **5**, e1000439 (2009).
[20] A. Boulbitch, B. Quinn, and D. Pink, Phys. Rev. Lett. **85**, 5246 (2000).
[21] See supplemental material at http://link.aps.org/supplemental/... for details regarding experimental methods and theoretical derivations.
[22] Circumferential quantities are denoted as $\perp$ while axial quantities are denoted as $\|$.
[23] The size and stiffness of a similar strain of *E. coli* that does not carry the *imp4213* mutation was within 10% of the values for the *imp-* strain, indicating that increased outer membrane permeability does not have a large effect on the turgor pressure or cell wall elasticity.
[24] S. Wang, H. Arellano-Santoyo, P. A. Combs, and J. W. Shaevitz, Proc Natl Acad Sci U S A **107**, 9182 (2010).